

A Kinetic Study of the Reaction between Ethylperoxy Radicals and HO₂

M. Matti Maricq* and Joseph J. Szente

Research Laboratory, Ford Motor Company, P.O. Box 2053, Drop 3083, Dearborn, Michigan 48121

Received: September 2, 1993; In Final Form: November 23, 1993*

Flash photolysis–time-resolved UV spectroscopy is used to measure the rate constant for the C₂H₅O₂ + HO₂ reaction over the temperature range of 210–363 K. The radicals are generated by photolysis of F₂ in the presence of H₂ and ethane. The rate constant for the F + C₂H₆ reaction is measured relative to the F + H₂ reaction to be $k_1 = (7.1^{+2.1}_{-1.6}) \times 10^{-10} e^{(-347 \pm 69)/T} \text{ cm}^3 \text{ s}^{-1}$. In order to ascertain time-resolved concentrations, the HO₂ UV absorption cross section and its self-reaction rate constant have been remeasured. The UV cross section is in good agreement with previous reports, with $\sigma_{\text{max}} = 0.041 \text{ \AA}^2$ at 203 nm. The self-reaction rate constant of $k_5 = (2.8 \pm 0.5) \times 10^{-13} e^{(594 \pm 55)/T} \text{ cm}^3 \text{ s}^{-1}$ is in excellent agreement with the currently recommended value. The rate constant for the C₂H₅O₂ + HO₂ reaction is $k_7 = (6.9^{+2.1}_{-1.6}) \times 10^{-13} e^{(702 \pm 69)/T} \text{ cm}^3 \text{ s}^{-1}$. This result is discussed with regard to the discrepancy which exists between the two previous measurements of this rate constant.

I. Introduction

The initial steps in the degradation of hydrocarbons released into the atmosphere are generally straightforward; the hydrocarbon is attacked by OH to form the corresponding alkyl radical, which then adds O₂ to form a peroxy radical. Subsequent degradation can follow a variety of pathways, for example, reaction with NO, HO₂, or another peroxy radical. In geographic regions with low NO_x concentrations, such as a rural environment, reaction with HO₂ can become the dominant pathway for the removal of organic peroxy radicals. Knowledge of RO₂ + HO₂ rate constants is also required for laboratory studies of peroxy radical chemistry, because of the fact that HO₂ is often formed as a secondary product, for example, via RO₂ + NO → RO + NO₂ followed by RO + O₂ → R'CHO + HO₂.

Relatively few studies of organic peroxy radical reactions with HO₂ have been reported in the literature.¹ The earlier measurements of ethylperoxy² and methylperoxy^{3,4} radical reactions with HO₂ yielded rate constants of the order $5 \times 10^{-12} \text{ cm}^3 \text{ s}^{-1}$ at 295 K and indicated a moderate negative temperature dependence with an $E_a \sim -600 \text{ K}$. More recently, investigations of the reaction between HO₂ and larger organic peroxy radicals, e.g. neopentyl⁵ and cyclohexylperoxy⁶ radicals, have shown enhanced rate constants at room temperature (approximately a factor of 3 faster) and a steeper temperature dependence ($E_a \sim -1300 \text{ K}$) as compared to the case for methyl or ethyl peroxy radicals.

Very recently, a new study of the C₂H₅O₂ + HO₂ reaction has been reported,⁷ in which the magnitude and temperature dependence of the rate constant are essentially identical to those for the larger organic peroxy radicals, such as the cyclopentylperoxy radical.⁶ This has led the authors to posit that methylperoxy radical, instead of serving as the example of a typical peroxy radical in its reactivity toward HO₂, should be considered the exception. However, the new C₂H₅O₂ + HO₂ results are in stark disagreement with the previous study² which showed the rate constant to have essentially the same magnitude and temperature dependence as for the CH₃O₂ + HO₂ reaction.

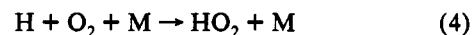
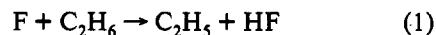
The present study aims to resolve the discrepancy in the two previous measurements. The experiments described herein differ from the earlier work in two ways:^{2,7} the use of F₂ photolysis in the presence of H₂ and ethane to produce the reactants and the use of time-resolved spectroscopy to determine HO₂ and C₂H₅O₂

concentration versus time profiles. The fitting of these concentration profiles to predictions from the appropriate kinetic model reveals the HO₂ + C₂H₅O₂ reaction to exhibit the moderate temperature dependence reported by Dagaut et al.,² as opposed to the steeper dependence found by Fenter et al.;⁷ however, the magnitude of the rate constant is approximately 60% larger than measured by Dagaut et al.

The paper is organized as follows. Section II presents an overview of the experimental method and the spectral deconvolution procedure. The UV spectrum of HO₂ and its self-reaction kinetics are discussed in section III. The title reaction forms the subject of section IV, which presents our experimental measurements and a comparison to previous work. The kinetics of the F + C₂H₆ reaction is the subject of section V.

II. Experimental Section

Time-resolved UV spectra of the HO₂ + C₂H₅O₂ reaction were obtained using the flash photolysis–UV spectrometer which has been previously described.^{8,9} The experiments are conducted by flowing a F₂/H₂/C₂H₆/O₂/N₂ gas mixture although a jacketed and insulated fused silica cell 3.2 cm in diameter by 51 cm in length. A 400–600-mJ pulse of 351-nm light from an excimer laser photolyses approximately 0.25% of the F₂ in the mixture to produce F atoms. These react rapidly via



to produce the starting HO₂ and C₂H₅O₂ populations. The hydrogen, ethane, and oxygen concentrations were chosen sufficiently large to ensure that the initial peroxy radicals are formed within a few microseconds of the photolysis pulse, a time scale fast compared to the ensuing peroxy radical reactions which occur over about 6 ms. The relative amount of H₂ to C₂H₆ was further adjusted to obtain the desired ratio of HO₂ to C₂H₅O₂ (typically 40%/60%).

The ethylperoxy and hydroperoxy radicals are detected through their UV absorption in the 200–250-nm range. Broadband UV light from a D₂ lamp counterpropagates the cell and is dispersed

* Author to whom correspondence should be addressed.

• Abstract published in *Advance ACS Abstracts*, January 15, 1994.

TABLE 1: UV Absorption Cross Sections

wavelength (nm)	$\sigma(\text{HO}_2)$ (10^{-18} cm^2)	wavelength (nm)	$\sigma(\text{HO}_2)$ (10^{-18} cm^2)
273.1	0.13	226.8	2.65
270.0	0.11	223.7	2.94
266.9	0.14	220.6	3.21
263.8	0.15	217.6	3.44
260.8	0.20	214.5	3.66
257.7	0.27	211.4	3.75
254.6	0.36	208.3	3.94
251.5	0.46	205.2	4.02
248.4	0.63	202.1	4.08
245.3	0.82	199.0	3.98
242.2	1.01	196.0	3.86
239.2	1.30	192.9	3.64
236.1	1.58	189.8	3.47
233.0	1.86	186.7	2.99
229.9	2.22		

by a 0.32-m monochromator with a 147 groove/mm grating onto a gated, intensified, diode array detector. Spectra are recorded at various times in the 0–6-ms range following the photolysis pulse. The spectral resolution is 2–3 nm, and the time resolution is 20 μs . The spectra are deconvoluted into time-dependent individual species concentrations via

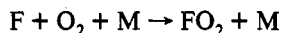
$$\text{Abs}(t) = [\text{HO}_2]_t \ell \sigma(\text{HO}_2) + [\text{C}_2\text{H}_5\text{O}_2]_t \ell \sigma(\text{C}_2\text{H}_5\text{O}_2)$$

where ℓ represents the path length and σ the wavelength-dependent cross section of the particular peroxy radical. Absolute UV cross sections for $\text{C}_2\text{H}_5\text{O}_2$ were reported in ref 8 and are in good agreement with the values reported by Fenter et al.⁷ We have remeasured the HO_2 spectrum in order that the two reference spectra are obtained using the same apparatus and optical path.

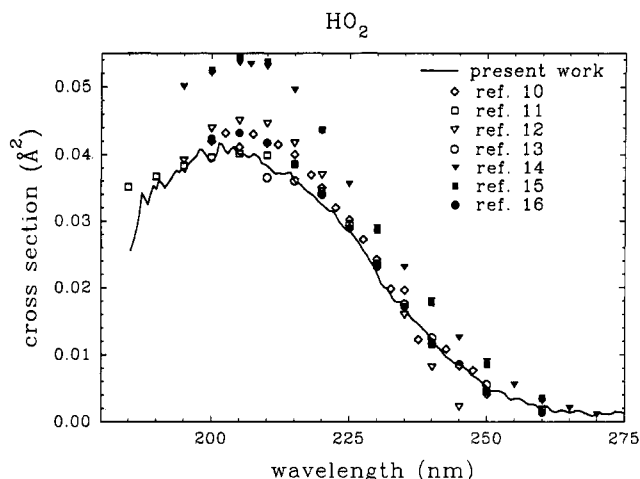
Temperature control is achieved using a Neslab ULT-80dd recirculating chiller which can be set between 210 and 363 K. The gases, except ethane, were recooled to a value within 10 K of set point before they entered the cell. Gas flow rates were regulated by Tylan flow controllers, except for F_2 , for which the flow was set by a needle valve. The individual gas concentrations were determined by timing their flows into a constant volume and equating the partial pressure to the corresponding fractional flow times the total pressure. A typical gas mixture consisted of 13 Torr H_2 , 2 Torr C_2H_6 , 34 Torr of 10% F_2/N_2 , 80 Torr O_2 , and sufficient N_2 to achieve a total pressure of about 200 Torr.

III. HO₂ UV Spectrum and Self-Reaction Kinetics

Hydroperoxy radicals were generated following photolysis of a $\text{F}_2/\text{H}_2/\text{O}_2/\text{N}_2$ gas mixture via reactions 2 and 4. The hydrogen and oxygen concentrations were increased until the absorption in the 200–250-nm range at 20 μs remained unchanged. The ratio of H_2/O_2 was kept above 1/7 in order to minimize the formation of FO_2 via



This is necessary because FO_2 absorbs light in the same spectral region as HO_2 , except with an intensity 3 times that of the latter. Absolute cross sections were determined by substituting ethane for H_2 , under otherwise identical experimental conditions, and determining the resultant $\text{C}_2\text{H}_5\text{O}_2$ concentration (produced from reactions 1 and 3) from its absorbance and literature UV cross section.⁸ This ethylperoxy concentration was equated to the initial F atom concentration and thereby the HO_2 concentration, except that the latter was corrected ($\sim 2\%$) for the loss of HO_2 by self-reaction in the 20- μs interval between photolysis and measurement of the spectrum. The UV cross sections obtained from the corrected concentration and measured absorbance are listed in Table 1. The spectrum is closely fit by a Gaussian lineshape, $\sigma = \sigma_{\text{max}} \exp(-b[\ln(\lambda_{\text{max}}/\lambda)]^2)$, with $\lambda_{\text{max}} = 204 \text{ nm}$, $\sigma_{\text{max}} = 0.041 \text{ \AA}^2$, and $b = 45$; however, the latter slightly overestimates the experimental cross sections over 240–260 nm and slightly underestimates them over 220–230 nm.

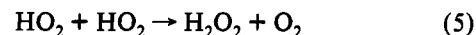
Figure 1. UV absorption spectrum of the HO₂ radical.TABLE 2: C₂H₅O₂ + HO₂ Reaction Mechanism

reaction ^a	rate constant k
1. $\text{F} + \text{C}_2\text{H}_6 \rightarrow \text{C}_2\text{H}_5 + \text{HF}$	$7.1 \times 10^{-10} e^{-347/T} \text{ cm}^3 \text{ s}^{-1} \text{ }^b$
2. $\text{F} + \text{H}_2 \rightarrow \text{H} + \text{HF}$	$1.7 \times 10^{-10} e^{-550/T} \text{ cm}^3 \text{ s}^{-1} \text{ }^{25}$
3. $\text{C}_2\text{H}_5 + \text{O}_2 + \text{M} \rightarrow \text{C}_2\text{H}_5\text{O}_2 + \text{M}$	$7 \times 10^{-12} \text{ cm}^3 \text{ s}^{-1} \text{ }^{25}$
4. $\text{H} + \text{O}_2 + \text{M} \rightarrow \text{HO}_2 + \text{M}$	$5.9 \times 10^{-32} \text{ cm}^6 \text{ s}^{-1} \text{ }^{17}$
5. $\text{HO}_2 + \text{HO}_2 \rightarrow \text{H}_2\text{O}_2 + \text{O}_2$	$2.8 \times 10^{-13} e^{594/T} \text{ cm}^3 \text{ s}^{-1} \text{ }^b$
6. $\text{C}_2\text{H}_5\text{O}_2 + \text{C}_2\text{H}_5\text{O}_2 \rightarrow \text{products}$	$9.1 \times 10^{-14} \text{ cm}^3 \text{ s}^{-1}$
7. $\text{C}_2\text{H}_5\text{O}_2 + \text{HO}_2 \rightarrow \text{C}_2\text{H}_5\text{OOH} + \text{O}_2$	$6.9 \times 10^{-13} e^{702/T} \text{ cm}^3 \text{ s}^{-1} \text{ }^b$

^a Reaction numbers correspond to those used in the text. ^b Measured in the present study.

Figure 1 compares the HO_2 spectrum measured in the present work to previously reported spectra.^{10–16} There is excellent agreement (within 10%) with the previous work, excluding the two sets of cross sections that are clearly too large. Our spectrum is 6% lower in intensity than the recent diode array—molecular modulation measurements of Crowley et al.¹⁶ (shown here as points averaged over 5 nm). The agreement is particularly good in the region below 220 nm where there has been the most disagreement between the earlier spectra. In fact, both spectral measurements peak at 203 nm. The estimated uncertainty in the present HO_2 cross section is approximately 10%, based on 5% uncertainty in the $\text{C}_2\text{H}_5\text{O}_2$ cross section and allowing 5% error due to small changes in experimental conditions incurred by substituting ethane for hydrogen.

The kinetics of HO_2 self-reaction were examined at various temperatures by measuring the HO_2 absorbance at various delay times following laser photolysis. Using a one-parameter fit of the absorbance to the reference spectrum discussed above, the absorbances were converted to concentrations. However, it was found that these concentrations did not decay to zero but instead approached a value approximately 10% of the initial radical concentration. The reason is that the H_2O_2 product of the self-reaction



itself exhibits a UV absorption. Its spectrum is somewhat blue shifted in comparison to that of HO_2 and is, on average, 10% as intense in the 190–250-nm range.¹⁷ Over this range, the shape of the H_2O_2 spectrum is sufficiently similar to that of HO_2 that, instead of yielding the HO_2 concentration, fitting of the time-resolved absorbances yields the “effective” concentration $[\text{HO}_2]_t + 0.1[\text{H}_2\text{O}_2]_t$. A comparison of these “effective” concentrations to predictions from a model given by reactions 2, 4, and 5 of Table 2 provides the temperature-dependent rate constants shown in Figure 2. The best fit of the rate constants to an Arrhenius expression yields $k_5 = (2.8 \pm 0.5) \times 10^{-13} e^{(594 \pm 55)/T} \text{ cm}^3 \text{ s}^{-1}$.

The activation energy, $E_a = 594 \text{ K}^{-1}$, is nearly identical to the currently recommended value^{18,17} of 600 K^{-1} , whereas the preexponential factor of $2.8 \times 10^{-13} \text{ cm}^3 \text{ s}^{-1}$ is slightly larger than

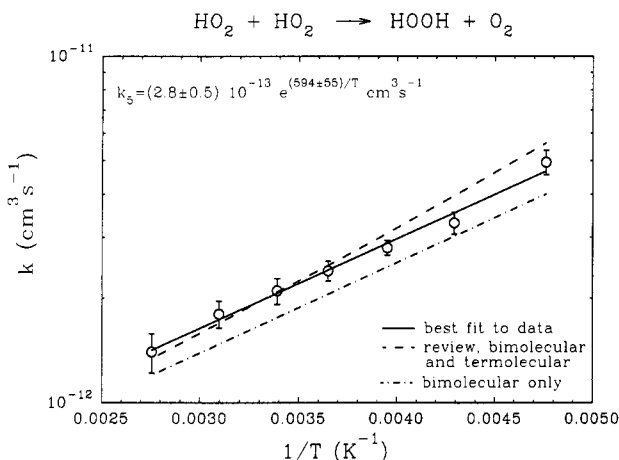


Figure 2. Rate constant versus temperature for the reaction $\text{HO}_2 + \text{HO}_2$.

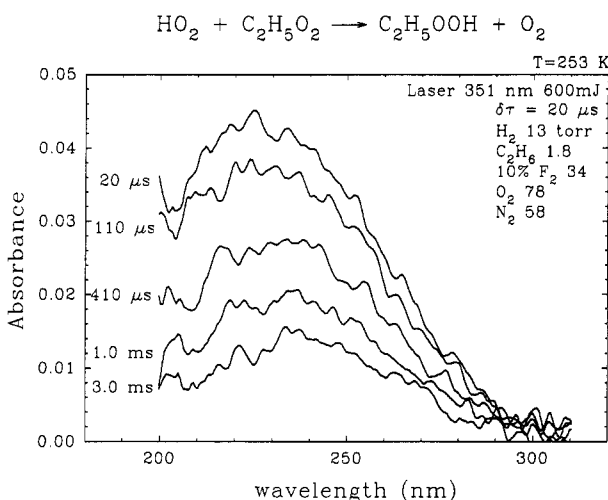


Figure 3. Time-resolved UV spectra of a $\text{F}_2/\text{H}_2/\text{C}_2\text{H}_6/\text{O}_2/\text{N}_2$ gas mixture at various times following flash photolysis of the F_2 .

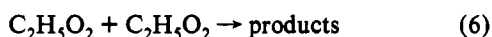
the recommendation of $2.3 \times 10^{-13} \text{ cm}^3 \text{ s}^{-1}$. This is because the literature expression for the HO_2 self-reaction rate constant,¹⁷

$$k_5 = 2.3 \times 10^{-13} e^{600/T} + 1.7 \times 10^{-33} [\text{air}] e^{1000/T} \text{ cm}^3 \text{ s}^{-1}$$

contains both bi- and termolecular components. At the $P_{\text{Tot}} = 200$ Torr of our experiments, $1.7 \times 10^{-33} [\text{air}] e^{400/T} \approx 0.43 \times 10^{-13}$ for $T = 295$ K, implying that the "effective" bimolecular preexponential factor is 2.73×10^{-13} , a value essentially identical to the one reported in this work. This agreement is also illustrated by the excellent fit (dashed line) of the literature recommendation to our data in Figure 2. The dot-dash line shows the predictions from the bimolecular component alone and indicates that the termolecular channel plays a minor ($\sim 10\%$) role at 200 Torr total pressure.

IV. $\text{HO}_2 + \text{C}_2\text{H}_5\text{O}_2$

The cross-reaction between hydroperoxy and ethylperoxy radicals was examined by time-resolved UV spectroscopy following the photolysis of F_2 in the presence of H_2 , C_2H_6 , and O_2 . Typical spectra are shown in Figure 3. The absorbance of the reacting mixture exhibits a decrease in intensity along with a concomitant shift to the red with increasing time. This can be explained as follows. HO_2 molecules are removed both by self-reaction and cross-reaction with $\text{C}_2\text{H}_5\text{O}_2$. Ethylperoxy radicals, on the other hand, are effectively removed only by the cross-reaction; the self-reaction



is too slow to be of significance over the 6-ms duration of the present measurements. Thus, the HO_2 radicals decay more

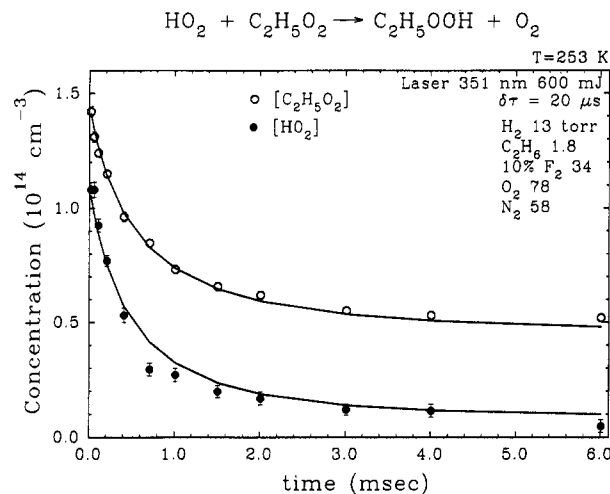


Figure 4. Concentration versus time profiles for HO_2 and $\text{C}_2\text{H}_5\text{O}_2$ obtained by deconvolution of the corresponding time-resolved UV spectra.

rapidly than their $\text{C}_2\text{H}_5\text{O}_2$ counterparts, and their contribution to the total absorbance, which peaks at 203 nm, diminishes more rapidly, leading to the observed red shift.

A two-parameter fit of the time-resolved absorption spectra to ethylperoxy and hydroperoxy reference spectra yields concentration versus time profiles such as those illustrated in Figure 4. Notice that the decrease in $[\text{C}_2\text{H}_5\text{O}_2]$ from 1.5×10^{14} to $0.5 \times 10^{14} \text{ cm}^{-3}$ almost matches the decay in $[\text{HO}_2]$, indicating the cross-reaction



to be the predominant radical loss mechanism. As was discussed in section III, however, the apparent HO_2 absorbance does not decay to zero but instead to a value equal to approximately 10% of the loss in $\text{C}_2\text{H}_5\text{O}_2$ (equivalently HO_2). As with H_2O_2 , the spectrum of CH_3OOH , and we assume $\text{C}_2\text{H}_5\text{OOH}$, has a shape similar to the spectrum of HO_2 over the range of 200–250 nm, except that the intensity is about 10 times smaller. Therefore, the data marked $[\text{HO}_2]$ in Figure 4 should be interpreted as the "effective" concentrations $[\text{HO}_2] + 0.1\{[\text{C}_2\text{H}_5\text{OOH}] + [\text{HOOH}]\}$.

The concentration versus time profiles are compared to the predictions from the model of Table 2 in order to fit the rate constant for the cross-reaction. Actually, reactions 1–4 occur over microsecond time scales; thus, the initial HO_2 and $\text{C}_2\text{H}_5\text{O}_2$ populations are formed essentially instantaneously on the time scale of their subsequent decay. As already mentioned, the ethylperoxy self-reaction is sufficiently slow to be of minor importance to the model predictions. Hence, the decay of HO_2 and $\text{C}_2\text{H}_5\text{O}_2$ radicals in Figure 4 depends on two rate constants, k_5 and k_7 . Because the HO_2 self-reaction rate constant was measured in a separate series of experiments, and is well-known from the literature, the challenge arises to fit simultaneously the HO_2 and $\text{C}_2\text{H}_5\text{O}_2$ decays with one adjustable parameter. It this can be accomplished successfully, it will lend weight to the validity of the reaction model.

The solid curves in Figure 4 illustrate the best fit of the model to the data. Recall that the data marked $[\text{HO}_2]$ actually include the H_2O_2 and $\text{C}_2\text{H}_5\text{OOH}$ concentrations as well. Without this interpretation, a simultaneous fit of the $[\text{C}_2\text{H}_5\text{O}_2]$ and $[\text{HO}_2]$ data is not possible, with the predicted HO_2 concentrations falling too rapidly when the $[\text{C}_2\text{H}_5\text{O}_2]$ data are well fit. Best fit values of k_7 are listed in Table 3 over the 210–363 K temperature range along with the experimental conditions under which they were obtained.

The error in k_7 arises predominantly from two sources, an error in fitting the concentration profiles to the model and the uncertainty in the initial concentrations (e.g. due to uncertainty in $\sigma(\text{HO}_2)$). A third, but smaller, source of error is the uncertainty in k_5 . For each experiment, two fits were performed, one to the

TABLE 3: C₂H₅O₂ + HO₂ and F + C₂H₆ Rate Constants

temp (K)	conditions ^a				[F] ₀	results ^b	
	C ₂ H ₆	H ₂	O ₂	total		k ₁	k ₇
210	1.7	13	76	178	3.0	1.45 ± 0.15	19 ± 4
210	1.7	13	75	178	2.8	1.4 ± 0.2	19 ± 5
210	1.5	10	67	178	6.0	1.5 ± 0.15	21 ± 4
210	1.3	10	66	176	3.8	1.2 ± 0.15	20 ± 4
233	1.7	13	77	181	2.6	1.7 ± 0.2	13 ± 4
233	1.6	11	70	185	6.2	1.6 ± 0.2	15 ± 5
243	1.8	23	79	180	2.6	1.5 ± 0.2	12 ± 2.4
243	1.8	5.9	82	190	2.9	1.3 ± 0.2	11 ± 2.4
253	1.7	13	77	182	2.6	1.9 ± 0.2	11.5 ± 2.6
253	1.8	13	78	185	2.6	1.9 ± 0.2	12.5 ± 3
253	1.5	10	70	182	4.1	1.9 ± 0.2	10.5 ± 1
273	1.8	13	80	189	2.8	2.2 ± 0.2	9.5 ± 1.3
295	1.8	14	82	193	2.6	2.3 ± 0.2	8.1 ± 1.5
295	1.9	13	87	690	2.9	2.0 ± 0.2	8.3 ± 1.5
295	1.5	10	70	190	3.6	2.5 ± 0.25	8.5 ± 1.3
323	1.9	14	84	202	3.3	2.6 ± 0.25	6.6 ± 1.4
323	2.0	13	89	698	2.5	2.6 ± 0.25	6.5 ± 1.2
323	1.7	12	75	192	6.1	2.5 ± 0.25	4.8 ± 1.4
338	1.9	25	87	195	3.6	2.3 ± 0.25	4.7 ± 1.0
338	2.0	6.5	90	206	3.7	2.1 ± 0.25	4.9 ± 1.1
363	1.9	12	77	201	5.6	2.7 ± 0.3	4.1 ± 1.0
363	2.0	15	87	209	3.0	3.1 ± 0.3	5.7 ± 1.2
363	2.1	13	87	209	1.7	2.8 ± 0.3	6.5 ± 1.4

^a Units are Torr, except for [F]₀ which is 10¹⁴ cm⁻³. ^b Units are 10⁻¹² cm³ s⁻¹ for k₇ and 10⁻¹⁰ cm³ s⁻¹ for k₁.

C₂H₅O₂ and the other to the HO₂ concentrations. In each case, the fit to the ethylperoxy data is substantially more sensitive to the value of k₇ than is the fit to the HO₂ concentrations. Typical fitting errors are 10% for the ethylperoxy data as compared to 20–30% for the HO₂ data. This is as expected because the ethylperoxy concentration depends only on the rate of cross-reaction whereas the HO₂ concentration depends both on this rate and on the rate of self-reaction. Although the sensitivity to k₇ is different, the fits to HO₂ and C₂H₅O₂ yield rate constants that agree with each other within their error bounds.

The initial C₂H₅O₂ and HO₂ radical concentrations measured following the photolysis of the F₂/H₂/C₂H₆/O₂/N₂ gas mixture were confirmed by measurements of the initial C₂H₅O₂ or HO₂ concentrations determined in the absence of H₂ or C₂H₆, respectively. In each case, it was verified that the total initial radical concentration, given by the latter measurements, was consistent with the sum of the peroxy radical concentrations determined from the mixture. There remains, owing to the uncertainties in C₂H₅O₂ and HO₂ UV cross sections, an error in partitioning the total initial radical concentration between the two species. In particular, the value of k₇ determined by fitting the ethylperoxy data is sensitive to the choice of HO₂ initial concentration. A 10% change in this quantity (as would occur by scaling our value¹⁹ of σ(HO₂) by ±10%) results in a 10–20% variation in the best-fit value of k₇. Statistically combining this error with the fitting error and a 5% error due to the uncertainty in k₅ yields the error bars reported in Table 3 and shown in Figure 5. The errors in rate constant determinations are also evident from the scatter of the data, which is within the reported error bounds.

While most of the experimental measurements of k₇ were carried out at P_{Tot} ≈ 200 Torr, a limited number were performed at 700 Torr. These results indicated the lack of a significant pressure dependence on k₇, in agreement with the findings of Dagaut et al.²

Most of the experiments were performed with an initial concentration ratio of [C₂H₅O₂]₀/[HO₂]₀ = 1.3. However, at 243 and 338 K the ratio was varied from about 0.6 to 2.1. No systematic effect of the initial radical concentration ratio on the measured value of k₇ was observed. In addition, variation of the total initial radical concentration from about 3 × 10¹⁴ cm⁻³ to 6 × 10¹⁴ cm⁻³ had no observable effect on the rate constant. We did observe, however, that groups of measurements made many

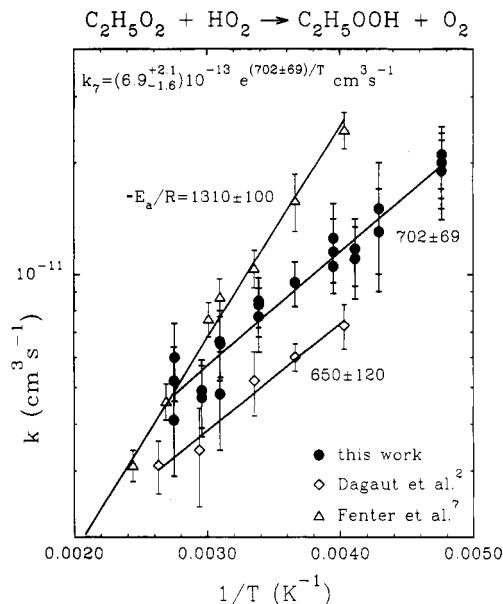


Figure 5. Rate constant versus temperature for the reaction C₂H₅O₂ + HO₂.

weeks apart sometimes showed small systematic increases or decreases in the values of the rate constant, where all the rate constants in the group had the same fractional change. For example, this can be seen in Figure 5 for the rate constants at 243 and 338 K. It is possible that slight variations in the H₂O impurity levels in the bath gas could explain this; however, since the deviations were within the signal to noise of the experiment, this matter was not pursued.

Figure 5 shows ln(k₇) vs 1/T plots of the rate constants reported herein and compares them to the results of the previous two studies. A best fit of our data to an Arrhenius expression yields

$$k_7 = (6.9_{-1.6}^{+2.1}) \times 10^{-13} e^{(702 \pm 69)/T} \text{ cm}^3 \text{ s}^{-1}$$

where 2σ error bars are indicated. Two features are immediately obvious from the figure. The temperature dependence of the rate constant is in excellent agreement with the results reported by Dagaut et al.;² however, the absolute magnitudes of the rate constants are approximately 60% higher. Part of this discrepancy can be attributed to the different HO₂ and C₂H₅O₂ UV cross sections used in the present as opposed to the earlier work. The present ethylperoxy cross sections are approximately 10% larger than those used by Dagaut et al. (at σ_{max}), whereas the earlier HO₂ spectrum extends only to 220 nm, where the ethylperoxy spectrum still has an intensity 65% of its maximum. It is estimated that these aspects can account for 20–30% of the 60% discrepancy between rate constant magnitudes. The remainder is possibly due to the fitting procedures which were employed; the individual concentration vs time profiles are directly fit to the reaction model in the present work as opposed to fitting the total absorbance at two wavelengths, as was done in the earlier work. The origin of the discrepancy between the present results and those of Fenter et al.⁷ is more puzzling. Because of the difference in temperature dependence, it cannot be due simply to a difference in the UV cross sections used in the fitting procedure. An explanation based on our use of F₂ photolysis and H₂ to produce HO₂ as opposed to Cl₂ photolysis in the presence of methanol is unlikely because of the similarity between our results and those of Dagaut et al.,² who also used the latter procedure to form HO₂.

V. F + C₂H₆

The photolysis of F₂ in the presence of H₂ and C₂H₆ initiates a competitive reaction between fluorine atoms and these two species, which in the presence of O₂ leads to the formation of HO₂ and C₂H₅O₂. We have used the initial ethylperoxy and

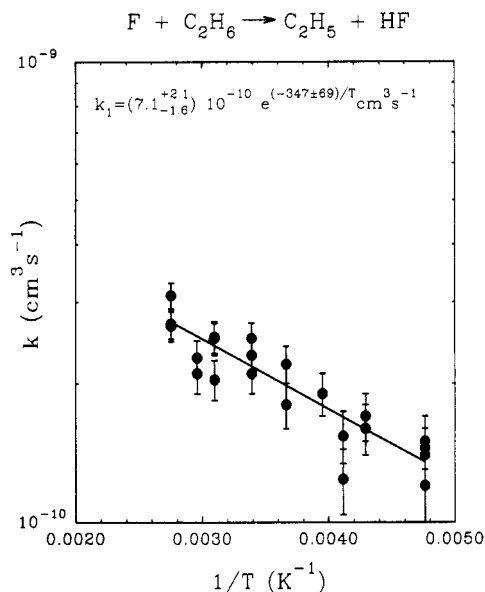


Figure 6. Rate constant versus temperature for the reaction $F + C_2H_6$.

hydroperoxy radical concentrations formed by the photolysis of an $F_2/H_2/C_2H_6/O_2/N_2$ gas mixture to determine temperature-dependent relative rate constants for the $F + C_2H_6$ reaction via

$$\frac{k_1}{k_2} = \frac{[C_2H_5O_2]_i [H_2]}{[HO_2]_i [C_2H_6]}$$

(a small correction is actually included to account for the $F + O_2$ reaction). The results are listed in Table 3 and shown in Figure 6.

The ($\sim 10\%$) error bars indicated for k_1 derive from the uncertainty in the relative HO_2 and $C_2H_5O_2$ UV cross sections and from the fitting error for the initial ethylperoxy and hydroperoxy radical concentration determinations. These error bars are consistent with the scatter in the data, as shown by Figure 6. One must add to this the systematic error due to uncertainty in the $F + H_2$ reaction, relative to which k_1 was measured.

The room-temperature value of $k_1 = 2.3 \times 10^{-10} \text{ cm}^3 \text{ s}^{-1}$ measured in the present work is in good agreement with the HF infrared chemiluminescence determination of $1.7\text{--}2.5 \times 10^{-10} \text{ cm}^3 \text{ s}^{-1}$ by Smith et al.,²⁰ the measurement relative to $F + H_2$ of $2.0 \times 10^{-10} \text{ cm}^3 \text{ s}^{-1}$ by Manning et al.,²¹ and the measurement relative to H_2 and CH_4 of $2.7 \times 10^{-10} \text{ cm}^3 \text{ s}^{-1}$ by Williams and Rowland.²² The present temperature-dependent rate constants are significantly larger than the earlier determinations of $7.9 \times 10^{-11} e^{-140/T} \text{ cm}^3 \text{ s}^{-1}$ by Ferris et al.²³ and $1.5 \times 10^{-11} e^{-240/T} \text{ cm}^3 \text{ s}^{-1}$ by Foon et al.²⁴ Note that the earlier work is also inconsistent with the more recent room-temperature measurements of k_1 discussed above.

The reaction between fluorine atoms and ethane is fast; $k_1 = (7.1_{-1.6}^{+2.1}) \times 10^{-10} e^{(-347 \pm 69)/T}$ (2σ error bars). In spite of this, it shows an activation barrier of approximately 0.7 kcal/mol. This barrier is very similar to that of $F + CH_4$, for which²⁵ $E_a = 0.8$ kcal/mol. However, the preexponential factor for the reaction with ethane is roughly 2 times larger than for methane. When chlorine atoms are substituted for fluorine, the reaction with ethane slows by about a factor of 4 at 295 K, but the activation barrier drops to near zero.²⁵

VI. Conclusion

Time-resolved UV spectroscopy has been applied to a study of the HO_2 absorption spectrum, its self-reaction kinetics, and its

reaction with ethylperoxy radicals. The UV absorption cross sections, while near the low end of the range of previously reported values, are in very good agreement with the majority of previous measurements. The self-reaction was investigated only in the low-pressure regime, in which the bimolecular channel dominates. Within this pressure regime, however, the measured rate constants are indistinguishable, within the experimental uncertainty, from the currently recommended values.^{17,18} These results serve two purposes. They verify previous measurements of the spectrum and reaction kinetics of an atmospherically important radical. Secondly, the good agreement with the literature values supports the accuracy of the experimental method when applied to the cross-reaction between ethylperoxy and hydroperoxy radicals.

The reinvestigation of the $HO_2 + C_2H_5O_2$ reaction has yielded a rate constant of $k_7 = 6.9 \times 10^{-13} e^{702/T} \text{ cm}^3 \text{ s}^{-1}$, which does not directly confirm either of the two previous studies. It being easier to reconcile a constant multiplicative factor between rate constant magnitudes as opposed to a difference in the temperature dependence of a rate constant, the present results would support the measurements of k_7 by Dagaut et al.² over those by Fenter et al.⁷ The temperature dependence found for the $HO_2 + C_2H_5O_2$ reaction is essentially the same as for the HO_2 self-reaction and for the $HO_2 + CH_3O_2$ reaction.^{3,4} This suggests that, in their reactivity with HO_2 , ethylperoxy radicals behave as "small" as opposed to "large" peroxy radicals such as neopentyl or cyclohexylperoxy radicals.

References and Notes

- Wallington, T. J.; Dagaut, P.; Kurylo, M. J. *Chem. Rev.* **1992**, *92*, 667.
- Dagaut, P.; Wallington, T. J.; Kurylo, M. J. *J. Phys. Chem.* **1988**, *92*, 3836.
- Lightfoot, P. D.; Veyret, B.; Lesclaux, R. *J. Phys. Chem.* **1990**, *94*, 708.
- Dagaut, P.; Wallington, T. J.; Kurylo, M. J. *J. Phys. Chem.* **1988**, *92*, 3833.
- Rowley, D. M.; Lesclaux, R.; Lightfoot, P. D.; Hughes, K.; Hurley, M. D.; Rudy, S.; Wallington, T. J. *J. Phys. Chem.* **1992**, *96*, 7043.
- Rowley, D. M.; Lesclaux, R.; Lightfoot, P. D.; Noziere, B.; Wallington, T. J.; Hurley, M. D. *J. Phys. Chem.* **1992**, *96*, 4889.
- Fenter, F. F.; Catoire, V.; Lesclaux, R.; Lightfoot, P. D. *J. Phys. Chem.* **1993**, *97*, 3530.
- Maricq, M. M.; Wallington, T. J. *J. Phys. Chem.* **1992**, *96*, 986.
- Maricq, M. M.; Szente, J. J. *J. Phys. Chem.* **1992**, *96*, 10862.
- Paukert, T. T.; Johnston, J. S. *J. Chem. Phys.* **1972**, *56*, 2824.
- Hochanadel, C. J.; Sworski, T. J.; Ogren, P. J. *J. Phys. Chem.* **1980**, *84*, 3274.
- Cox, R. A.; Burrows, J. P. *J. Phys. Chem.* **1979**, *83*, 2560.
- Kurylo, M. J.; Wallington, T. J.; Ouellette, P. A. *J. Photochem.* **1987**, *39*, 201.
- Moortgat, G. K.; Veyret, B.; Lesclaux, R. *J. Phys. Chem.* **1989**, *93*, 2362.
- McAdam, K.; Veyret, B.; Lesclaux, R. *Chem. Phys. Lett.* **1987**, *133*, 39.
- Crowley, J. M.; Simon, F.-G.; Burrows, J. P.; Moortgat, G. K.; Jenkin, M. E.; Cox, R. A. *J. Photochem. Photobiol. A: Chemistry* **1991**, *60*, 1.
- DeMore, W. B.; Sander, S. P.; Golden, D. M.; Hampton, R. F.; Kurylo, M. J.; Howard, C. J.; Ravishankara, A. R.; Kolb, C. E.; Molina, M. J. *Chemical Kinetics and Photochemical Data for Use in Stratospheric Modeling*; JPL publication 92-20, 1992.
- Atkinson, R.; Baulch, D. L.; Cox, R. A.; Hampson, R. F., Jr.; Kerr, J. A.; Troe, J. *J. Phys. Chem. Ref. Data* **1992**, *21*, 1125.
- Because k_7 is considerably more sensitive to the decay in ethylperoxy concentration as opposed to that of HO_2 , the effect of the uncertainty in $\sigma(HO_2)$ on the value of k_7 occurs primarily through the determination of the initial HO_2 concentration and not its subsequent decay.
- Smith, D. J.; Setser, D. W.; Kim, K. C.; Bogan, D. J. *J. Phys. Chem.* **1977**, *81*, 898.
- Manning, R. G.; Grant, E. R.; Merrill, J. C.; Parks, W. J.; Root, J. W. *Int. J. Chem. Kinet.* **1975**, *7*, 39.
- Williams, R. L.; Rowland, F. S. *J. Phys. Chem.* **1973**, *77*, 301.
- Fettis, G. C.; Knox, J. H.; Trotman-Dickenson, A. F. *J. Chem. Soc.* **1960**, 1064.
- Foon, R.; Reid, G. P.; Tait, K. B. *J. Chem. Soc. Faraday Trans. 1* **1972**, *68*, 1131.
- Westley, F.; Herron, J. T.; Cvetanovic, R. J.; Hampson, R. F.; Mallard, W. G. *NIST Chemical Kinetics Database*; NIST: Gaithersburg, 1991.